Modified generalized Brillouin zone theory with on-site disorder

Hongfang Liu,[1,2,3] Ming Lu,[4,*] Zhi-Qiang Zhang,[1,2,†] and Hua Jiang[1,2]
[1]*School of Physical Science and Technology, Soochow University, Suzhou 215006, China*
[2]*Institute for Advanced Study, Soochow University, Suzhou 215006, China*
[3]*Jiangsu Key Laboratory of Thin Films, Soochow University, Suzhou 215006, China*
[4]*Beijing Academy of Quantum Information Sciences, Beijing 100193, China*

(Received 2 January 2023; revised 24 March 2023; accepted 11 April 2023; published 24 April 2023)

We study the characterization of the non-Hermitian skin effect (NHSE) in non-Hermitian systems with on-site disorders. We extend the applications of generalized Brillouin zone (GBZ) theory to these systems. By proposing a modified GBZ theory, we give a faithful description of the NHSE. For applications, we obtain a unified β for system with long-range hopping and explain the GBZ irrelevance of the magnetic suppression of the NHSE in the previous study.

DOI: 10.1103/PhysRevB.107.144204

I. INTRODUCTION

Systems described by non-Hermitian Hamiltonians have been attracting intensive attention in recent years [1–81]. Many interesting phenomena have been reported [40–80], among which the non-Hermitian skin effect (NHSE) [55–81] has been the focus. The existence of the NHSE indicates that the conventional bulk-boundary correspondence (BBC) fails [55–59]. Meanwhile, the bulk spectrum shows distinct features for the open boundary (OBC) and periodic boundary (PBC) conditions, showing the collapse of the BBC. To accomplish the BBC, the generalized Brillouin zone (GBZ) theory [55,57,58] introduces a similarity transformation for the Hamiltonian, which eliminates the NHSE.

Nevertheless, a recent study [37] showed that the conventional GBZ theory fails to capture the features of the NHSE for samples under a magnetic field where the BBC still holds. Loosely speaking, such a model can be considered a one-dimensional model with an on-site disorder [82–84]. Very recently, the modified GBZ theory for disordered samples was reported [36], which breaks the limitation of the translational invariance required by the conventional GBZ theory. The essence of the modified GBZ theory is to find the minimum of a polynomial $\mathcal{F}(E,\beta) = |\det[E - \mathcal{H}_{\mathrm{PBC}}(\beta)] - \det[E - \mathcal{H}_{\mathrm{OBC}}]|$. However, applying the modified GBZ theory for samples with on-site disorder is still unreported, which leaves the GBZ irrelevance of the magnetic suppression of NHSE unsolved. Thus, there is an urgent need to study the influences of on-site disorders on the GBZ theory.

In this paper, we give a faithful characterization of NHSEs for samples with on-site disorders based on the modified GBZ theory. We uncover that the transformation coefficient $\beta = \beta_{\min}$ determined by the minimum of the polynomial $\mathcal{F}(E,\beta)$ gives an interval instead of a single point. To unify the description of NHSEs, we demonstrate that the modified GBZ theory also requires the minimization of $|\beta_{\min} - 1|$. Based on these considerations, we clarify the applicability of the GBZ theory in several prototypical disordered non-Hermitian models. Explicitly, a unified transformation coefficient $\beta_{\min}$ to achieve the global BBC for disordered samples with long-range hopping is obtained. A faithful description of NHSEs for samples under the magnetic field is also clarified, which removes the ambiguity of the GBZ irrelevance reported there.

II. MODEL AND METHOD

We start from the disordered Hatano-Nelson model [85] with the Hamiltonian:

$$\mathcal{H} = \sum_i \varepsilon_i c_i^\dagger c_i + t^+ c_i^\dagger c_{i+1} + t^- c_{i+1}^\dagger c_i, \tag{1}$$

where $c_i^\dagger$ (c_i) is the creation (annihilation) operator on the site i. Here, $t^\pm = (t \pm \gamma)$ represents the nearest-neighbor hopping, and γ encodes the non-Hermitian strength. We fix $t = 1$. Here, $\varepsilon_i \in [-W/2, W/2]$ denotes the on-site disorder [86] with W the disorder strength. The Hamiltonian under OBC and PBC are marked as $\mathcal{H}_{\mathrm{OBC}}$ and $\mathcal{H}_{\mathrm{PBC}}$, respectively.

Following the modified GBZ theory [36], we adopt the transformation $t^\pm \to t^\pm \beta^{\pm 1}$. Here, β is the transformation coefficient, which gives a quantitative description of the NHSE [36,55,58]. The transformed Hamiltonian under PBC [$\mathcal{H}_{\mathrm{GBZ}} \equiv \mathcal{H}_{\mathrm{PBC}}(\beta)$] satisfies [36]

$$\det[E - \mathcal{H}_{\mathrm{GBZ};N\times N}] = \det[E - \mathcal{H}_{\mathrm{OBC};N\times N}] + f_{\mathrm{PBC}}, \tag{2}$$

where $f_{\mathrm{PBC}} = t^+ t^- \det[E - \mathcal{H}_{\mathrm{OBC};N-2\times N-2}] + (t^+)^N \beta^N + (t^-)^N \beta^{-N}$. Here, N denotes the size of the Hamiltonian, and E is the eigenvalue of $\mathcal{H}_{\mathrm{OBC};N\times N}$. We mark $\mathcal{F}(E,\beta) = |\det[E - \mathcal{H}_{\mathrm{PBC}}(\beta)] - \det[E - \mathcal{H}_{\mathrm{OBC}}]|$ as follows:

$$\mathcal{F}(E,\beta) \equiv |f_{\mathrm{PBC}}| = |\mathcal{F}_1 + \mathcal{F}_2|, \tag{3}$$

*luming@baqis.ac.cn
†zhangzhiqiangphy@163.com

where $\mathcal{F}_1 = t^+t^- \det[E - \mathcal{H}_{\mathrm{OBC};N-2\times N-2}]$ and $\mathcal{F}_2 = (t^+)^N\beta^N + (t^-)^N\beta^{-N}$. For $W = 0$, one should notice $\mathcal{F}_1$ is negligible where $\det[E - \mathcal{H}_{\mathrm{OBC};N\times N}] = 0$ and $\det[E - \mathcal{H}_{\mathrm{OBC};N-2\times N-2}] \approx 0$ [36]. The modified GBZ theory requires the minimum of $\mathcal{F}(E,\beta) = |\mathcal{F}_2|$, which gives rise to $\beta_{\min} = \sqrt{|t^-/t^+|}$, consistent with the conventional GBZ theory [55,58]. Here, $\beta = \beta_{\min}$ gives the minimum of the polynomial $\mathcal{F}(E,\beta)$.

In fact, $\min[\mathcal{F}(E,\beta)]$ is the requirement to implement the BBC in non-Hermitian systems. The key for the BBC is to ensure the following equation [36]:

$$\det[E - \mathcal{H}_{\mathrm{OBC}}] \equiv \det[E - \mathcal{H}_{\mathrm{OBC}}(\beta)] \approx \det[E - \mathcal{H}_{\mathrm{PBC}}(\beta)]. \tag{4}$$

Notably, the NHSE leads to $\det[E - \mathcal{H}_{\mathrm{OBC}}] \not\approx \det[E - \mathcal{H}_{\mathrm{PBC}}]$, since $|\det[E - \mathcal{H}_{\mathrm{PBC}}]|$ is significantly enhanced due to the asymmetric hopping. It corresponds to the breakdown of the BBC for $\mathcal{H}$. To approach the BBC by adopting $\mathcal{H}_{\mathrm{PBC}}(\beta)$ [36,55], $\mathcal{H}_{\mathrm{PBC}}(\beta)$, and $\mathcal{H}_{\mathrm{OBC}}$ should have a similar eigenvalue E, which means $|\det[E - \mathcal{H}_{\mathrm{PBC}}(\beta)]|$ should tend to approach $|\det[E - \mathcal{H}_{\mathrm{OBC}}]|$. Thus, the BBC problem can be considered a problem of finding the minimum of $\mathcal{F}(E,\beta) = |\det[E - \mathcal{H}_{\mathrm{PBC}}(\beta)] - \det[E - \mathcal{H}_{\mathrm{OBC}}]|$ in general [36].

In the following, we apply the modified GBZ theory for samples with on-site disorders. When disorder is strong enough, we demonstrate that $\mathcal{F}_1$ has considerable influence on achieving the appropriate characterization of the NHSE since $[\mathcal{F}_1(E)]/\min[|\mathcal{F}_2(\beta)|] \propto [(E - \varepsilon_i)/t]^N$. We have to emphasize that $\mathcal{F}_1$ can be neglected for samples with hopping disorder in our previous study [36] since NHSEs are mostly contributed from eigenstates near $E = 0$ for considerable disorder strength. Noticing $[\mathcal{F}_1(E)]/\min[|\mathcal{F}_2(\beta)|] \propto (E/t)^N \sim 0$, it is reasonable to neglect $\mathcal{F}_1$ in our previous study [36]. Notably, for the weak disorder strength, $\mathcal{F}_1$ is always negligible.

For illustration purposes, we first consider $t \sim \gamma$, where the Hamiltonian $\mathcal{H}_{\mathrm{OBC};m\times m}$ is roughly a triangular matrix. The eigenvalue of $\mathcal{H}_{\mathrm{OBC};m\times m}$ can be considered to satisfy $E_{\mathrm{OBC};m} \in \{E_i\} \approx \{\varepsilon_1, \varepsilon_2, \ldots, \varepsilon_i, \ldots, \varepsilon_m\}$ with $E_{\mathrm{OBC};m} \in [-W/2, W/2]$. For $|W/2| > |t^{\pm}|$ and the thermodynamic limit $N \to \infty$, $\mathcal{F}_1 = t^+t^- \det[E - \mathcal{H}_{\mathrm{OBC};N-2\times N-2}]$ can be rewritten as

$$\mathcal{F}_1 \approx \prod_{i=1}^{N-2}(E - E_i)t^+t^- \approx \prod_{i=1}^{N}(E - E_i). \tag{5}$$

Here, $E_i \in E_{\mathrm{OBC};N-2}$ is the eigenvalue of $\mathcal{H}_{\mathrm{OBC};N-2\times N-2}$. By considering the differences of the eigenvalues between $\mathcal{H}_{\mathrm{OBC};N\times N}$ and $\mathcal{H}_{\mathrm{OBC};N-2\times N-2}$, the analytical formula of $\mathcal{F}_1$ is obtained [see the Appendix A for more details]:

$$\mathcal{F}_1 = \left[\left(E - \frac{W}{2}\right)^{[(1/2)-(E/W)]} \times \left(E + \frac{W}{2}\right)^{[(1/2)+(E/W)]} e^{-1}\right]^N. \tag{6}$$

As plotted in Fig. 1(a), $|\mathcal{F}_1| \sim 2^N$ for $E = \frac{W}{2}$, which is comparable with $\mathcal{F}_2$. Thus, $\mathcal{F}_1$ should have distinct influences and cannot be neglected.

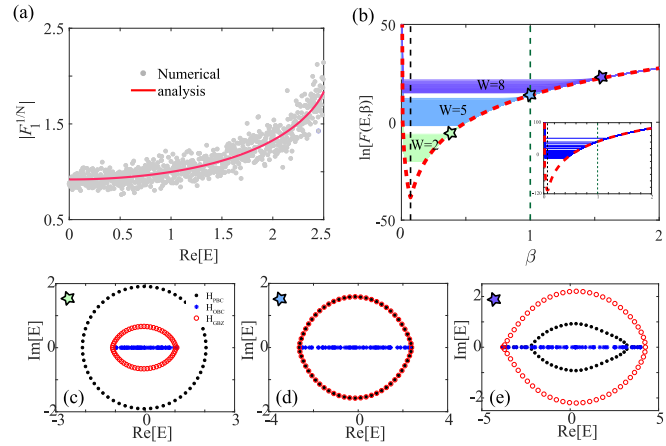

FIG. 1. (a) The analytical (red line) and numerical (gray dots) results of $|\mathcal{F}_1^{1/N}|$ vs the eigenvalue E for $W = 5$. (b) $\ln[\mathcal{F}(E,\beta)]$ vs β for different eigenvalues with $E \in [-W/2, W/2]$ under disorder strengths: $W = 2$ (green), $W = 5$ (blue), and $W = 8$ (purple). Pentagrams mark the right boundary of the plateaus for $E = \frac{W}{2}$. The red dashed line is the plot of $\ln[|\mathcal{F}_2|]$ for clean samples. Inset is the numerical results for $\mathcal{F}(E,\beta) = |\det[E - \mathcal{H}_{\mathrm{PBC}}(\beta)] - \det[E - \mathcal{H}_{\mathrm{OBC}}]|$ with $W = 8$. The real part $\mathrm{Re}[E]$ vs the imaginary part $\mathrm{Im}[E]$ of the eigenvalues E for (c) $W = 2$, (d) $W = 5$, and (e) $W = 8$. β for $\mathcal{H}_{\mathrm{GBZ}}$ is marked in (b). Other parameters are set as $\gamma = 0.99$ and $N = 60$.

To better understand the influence of $\mathcal{F}_1$, we plot $\mathcal{F}(E,\beta)$ vs β based on our analytical results, shown in Fig. 1(b). By neglecting $\mathcal{F}_1$ in Eq. (3), the minimum of $\mathcal{F}(E,\beta) = |\mathcal{F}_2| = |(t^+)^N\beta^N + (t^-)^N\beta^{-N}|$ and $\beta_{\min}$ are W and E independent. After considering $\mathcal{F}_1$, the global minimum of $\mathcal{F}(E,\beta) = |\mathcal{F}_1 + \mathcal{F}_2|$ is still $\beta_{\min} = \sqrt{|t^-/t^+|}$. Nevertheless, $\mathcal{F}(E,\beta)$ vs β gives rise to some plateaus, which is distinct from the result for clean samples [red dashed line in Fig. 1(b)]. Moreover, the value of the plateau roughly equals the global minimum $\mathcal{F}(E, \sqrt{|t^-/t^+|})$. Such a feature is also identified by numerical calculations directly based on Eq. (3), as shown in the inset of Fig. 1(b). Due to the existence of the plateau for $\mathcal{F}(E,\beta)$, $\beta_{\min}$ should be extended from a single point $\beta_{\min} = \sqrt{|t^-/t^+|}$ to an interval $\beta_{\min} \in [\Delta^-, \Delta^+]$ for a specific eigenvalue E. Here, $\Delta^{\pm}$ is determined at the boundary of the plateau.

Since $\beta_{\min} \in [\Delta^-, \Delta^+]$ roughly gives the same value $\mathcal{F}(E,\beta_{\min})$, all $\beta_{\min}$'s in the interval can be adopted to realize the BBC with considerable accuracy, and every $\beta_{\min}$ gives a correct description of the NHSEs. Nevertheless, to compare the NHSE for different cases, we demonstrate that the best choice of $\beta_{\min}$ should satisfy two key points: (1) It should be in the range $\beta_{\min} \in [\Delta^-, \Delta^+]$, which captures a correct description of the NHSEs; (2) $\beta_{\min}$ is the one closest to $\beta = 1$, i.e., $|\beta_{\min} - 1|$ has the minimum value.

Physically, the criterion of BBC ensures [36,55]

$$\begin{aligned} \mathcal{H}_{\mathrm{OBC}}\psi_n &= E_n\psi_n; \\ \mathcal{H}_{\mathrm{PBC}}(\beta_{\min})\widetilde{\psi}_n(\beta_{\min}) &= E_n\widetilde{\psi}_n(\beta_{\min}); \\ \psi_n &\approx S\widetilde{\psi}_n(\beta_{\min}). \end{aligned} \tag{7}$$

Here, $S = \mathrm{diag}[\beta_{\min}, \beta_{\min}^2, \ldots, \beta_{\min}^N]$ is a diagonal similarity transformation matrix. For a specific non-Hermitian sample,

the wave function ψ_n is determined. In the clean limits, $\widetilde{\psi}_n(\beta_{\min})$ is always an extended state. Conversely, for dirty samples, $\widetilde{\psi}_n(\beta_{\min})$ goes from extended to localized by varying $\beta_{\min}$ due to on-site disorders. Thus, the corresponding $\beta_{\min}$ expands to an interval to restore the original extensibility of $\widetilde{\psi}_n(\beta_{\min})$, where $\psi_n \approx S\widetilde{\psi}_n(\beta_{\min})$ still holds. Notably, $\beta_{\min}$ satisfying $\min|\beta_{\min}-1|$ gives rise to the most likely extended $\widetilde{\psi}_n(\beta_{\min})$, which is close to the clean limits. Additionally, when the NHSE is absent, one always has $\beta = 1$. Therefore, we suggest adopting the $\beta_{\min}$ satisfying $\min|\beta_{\min}-1|$ as the best depiction of the NHSEs.

These characteristics can be identified by $\mathcal{F}(E,\beta)$ and the plot of eigenvalues for different disorder strength W, as shown in Figs. 1(b)–1(e). Based on the proposed theory, one anticipates the NHSE being destroyed when the right boundary of the plateau [Δ^+ marked by pentagram] crosses the critical value $\beta = 1$. Such a feature is confirmed by the spectra shown in Figs. 1(c)–1(e). Generally, the eigenvalues have the NHSE if they form a closed loop with nonzero area in the complex energy plane under PBC (black dots) [61]. When the eigenvalues of $\mathcal{H}_{\text{PBC}}$ and $\mathcal{H}_{\text{OBC}}$ overlap, the corresponding eigenstates are localized due to disorder. For clarity, we focus on the eigenvalue $E = \frac{W}{2}$.

According to our analytical results shown in Fig. 1(b), $W = 5$ gives the critical point, and the eigenvalues of $\mathcal{H}_{\text{PBC}}$ and $\mathcal{H}_{\text{OBC}}$ should overlap with $\beta_{\min} = 1$. For $W < 5$, the BBC requires $\beta_{\min} < 1$, implying the existence of the NHSE for such an eigenvector. It is consistent with the plot in Fig. 1(c). When $W = 5$, the eigenvalues of $\mathcal{H}_{\text{OBC}}$ and $\mathcal{H}_{\text{PBC}}$ [$\beta_{\min} = 1$] overlap, as shown in Fig. 1(d). By further increasing W, the tails of the eigenvalues for $\mathcal{H}_{\text{PBC}}$ exist [see Fig. 1(e)], and the correlated eigenstates are localized. However, the BBC for $E = \frac{W}{2}$ remains available by adopting $\beta_{\min} \sim 1.5$. In the clean limits, $\beta_{\min} \neq 1$ predicts the existence of the NHSE. It naively gives an inappropriate description of the NHSE, where ψ_n and $S\widetilde{\psi}_n(\beta_{\min})$ have no NHSEs. Thus, a faithful characterization of the NHSE should minimize $|\beta_{\min}-1|$ for $\beta_{\min} \in [\Delta^-, \Delta^+]$ because, based on the modified GBZ theory, the localization features are captured by the plot of $\mathcal{F}(E,\beta)$ at $\beta = 1$, as shown in Fig. 1(b).

III. UNIFIED TRANSFORMATION COEFFICIENT FOR DISORDERED SAMPLES WITH NEXT-NEAREST-NEIGHBOR HOPPING

In previous section, we found that $\beta_{\min}$ is extended from a single point to an interval for achieving the BBC for disordered samples. As an application of such a feature, a unified transformation coefficient β is available for samples with long-range hopping even though it does not exist under the clean limits.

We focus on samples with next-nearest-neighbor hopping, shown in Fig. 2(a). Its Hamiltonian reads

$$\mathcal{H} = \sum_i \varepsilon_i c_i^\dagger c_i + t^{\pm} c_i^\dagger c_{i\pm1} + t c_i^\dagger c_{i\pm2}. \tag{8}$$

When disorder is absent ($W = 0$), $\beta_{\min}$ can be accurately determined, and the plot of $\text{Re}(\beta)$ vs $\text{Im}(\beta)$ forms a closed loop, as shown in the red curve in Fig. 2(b). Clearly, a unified transformation coefficient $|\beta_{\min}|$ to achieve the global BBC

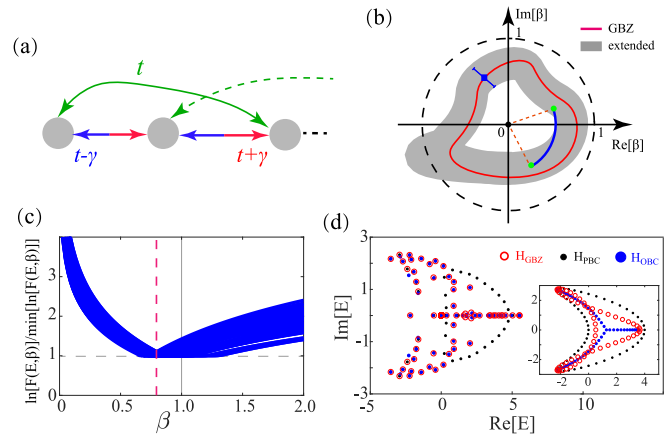

FIG. 2. (a) Schematic diagram of the model with next-nearest-neighbor hopping (green lines). (b) The schematic plots of $\text{Re}[\beta_{\min}]$ vs $\text{Im}[\beta_{\min}]$ for clean (red solid line) and disordered samples (area in gray). The disorder effect leads to the broadening of $\beta_{\min}$ marked by the error bar. Thus, a unified $|\beta|$ is available as marked with the blue solid line. (c) $\ln[\mathcal{F}(E,\beta)]/\min\{\ln[\mathcal{F}(E,\beta)]\}$ vs β for disorder strength $W = 7$. The red dashed line presents the overlap of $\beta_{\min}$ for different eigenvalues. (d) $\text{Re}[E]$ vs $\text{Im}[E]$ under periodic boundary conditions (PBC; black dots), open boundary conditions (OBC; blue dots), and generalized Brillouin zone (GBZ; PBC with $\beta = 0.77$ [red dashed line in (c)]; red circles). Inset is the plot for clean samples with $\beta \approx 0.854$, which gives rise to the bulk-boundary correspondence (BBC) for $E \approx -0.2 \pm 1.6i$. We fix $t = 1$, $\gamma = 1.4$, and $N = 60$.

does not exist [55,57], where $\beta_{\min}$ is E dependent. For a typical energy $E = E_0$, $\beta_{\min}(E_0)$ only ensures the BBC for such a state [see the inset of Fig. 2(d) as an example]. Thus, a global BBC cannot be obtained by simply utilizing a specific $\beta_{\min}(E)$ for the clean samples.

Nevertheless, after considering the disorder effect, the broadening of $\beta_{\min}$ will significantly alter the plot of $\text{Re}(\beta)$ vs $\text{Im}(\beta)$. To identify the unified transformation coefficient, we calculate the $\mathcal{F}(E,\beta)$ vs β for each eigenvalue E. As shown in Fig. 2(c), the interval of $\beta_{\min}(E)$ is determined by requiring $\ln\{\mathcal{F}(E,\beta_{\min})\}/\min\{\ln[\mathcal{F}(E,\beta_{\min})]\} \approx 1$. Remarkably, all $\beta_{\min}(E)$'s intersect at a single point, i.e., $\cap_{i\in E}\beta_{\min}(i) = 0.77$. Since $\beta_{\min}(E)$ ensures the BBC for the eigenvalue E, the transformed Hamiltonian $\mathcal{H}_{\text{GBZ}}$ with $\beta = 0.77$ will capture all the eigenvalues under OBC [see Fig. 2(d)]. The interplay between disorder effect and the BBC unveils one of the exotic properties of non-Hermitian systems.

IV. APPLICATION OF THE MODIFIED GBZ THEORY UNDER MAGNETIC FIELD

In this section, we apply the modified GBZ theory to the system with a magnetic field. The Hamiltonian reads

$$\mathcal{H} = \sum_{x,y} t^{\pm} c_{x,y}^\dagger c_{x\pm\delta_x,y} + t_y e^{\pm i\phi x} c_{x,y}^\dagger c_{x,y\pm\delta_y}. \tag{9}$$

Here, ϕ represents the magnetic flux. Recently, Lu *et al.* [37] and Shao *et al.* [38] noticed that the strength of the NHSE is significantly suppressed by increasing ϕ. However, the strength of the NHSE under the magnetic field cannot be

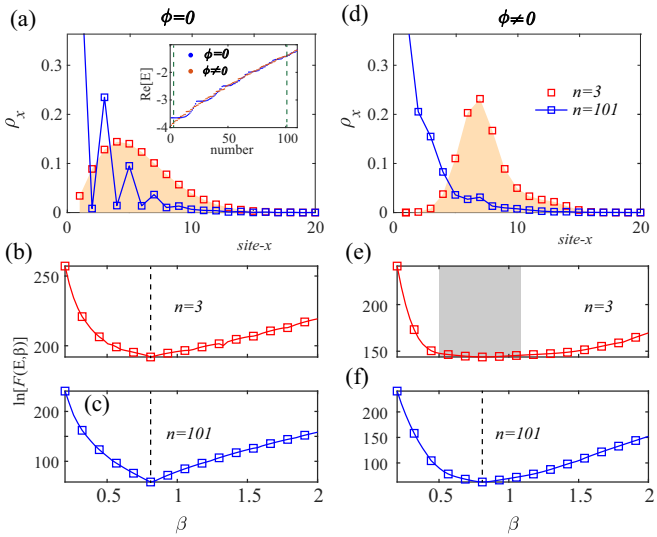

FIG. 3. (a) The plot of eigenstates $\rho_{x;n} = \sum_y |\psi_n(x, y)|^2$ vs site x for $n = 3$ and 101 with $\phi = 0$. Inset plots the real eigenvalues (Re[E]) for $\phi = 0$ (blue dots) and $\phi = 2\pi/(N-1)$ (red dots), which determines the choices of n. (b) and (c) $\mathcal{F}(E_n, \beta)$ vs β for $n = 3$ and 101, respectively. (d)–(f) are the same as (a)–(c), except $\phi = 2\pi/(N-1)$. We set $t^+ = 1.2, t^- = 0.8, t_y = 1$, and $N_x = N_y = N = 20$.

correctly described by the conventional GBZ theory [37]. The conventional GBZ theory seems to indicate that the NHSE is irrelevant to the magnetic field. Since such a model is closely related to a one-dimensional model with on-site disorder [82–84] [see the Appendix B for more details], we next elucidate that a faithful description of the NHSE is still available based on the proposed modified GBZ theory.

Significantly, the eigenequation gives rise to $\mathcal{H}\psi_n = E_n\psi_n(x, y)$. Here, E_n stands for the nth eigenvalue shown in the inset of Fig. 3(a). For clarity, we take $n = 3$ and 101 as two typical examples. To unveil the universality of the modified GBZ theory under magnetic field, we pay attention to the evolution of $\mathcal{F}(E_n, \beta)$ vs β. When the magnetic field is absent, the eigenvectors for $n = 3$ and 101 should both show the features of the NHSE, where a single point of $\beta_{\min} \sim 0.81$ is obtained [see $\mathcal{F}(E_n, \beta)$ in Figs. 3(b)–3(c)]. After considering the influence of ϕ, we notice that $\mathcal{F}(E_n, \beta)$ gives a plateau for $n = 3$ with $\beta_{\min} \in [0.5, 1.1]$. Based on the modified GBZ theory, $\beta_{\min} = 1$ should be adopted to characterize the NHSE, and the NHSE for $n = 3$ should be destroyed. On the contrary, a single point with $\beta_{\min} \sim 0.81$ is still available for $n = 101$. These results are consistent with the plot of eigenvectors in Figs. 3(a) and 3(d). The NHSE for $n = 3$ is destroyed with $n = 101$ unaffected by increasing ϕ, which manifests the magnetic-field-suppressed NHSE.

We close this section by clarifying why the GBZ theory fails to describe the NHSE. The modified GBZ theory considers the influence of $\mathcal{F}_1$ on the polynomial $\mathcal{F}(E, \beta)$, which smoothes its sharp dip. Nevertheless, such a process leaves the global minimum of $\mathcal{F}(E, \beta)$ unaffected. The applied GBZ theory in the previous study [37] only concentrated on the global minimum, which is almost unaffected by the magnetic field [see Fig. 3(e), the global minimum still gives $\beta \sim 0.8$]. However, the plateau of $\mathcal{F}(E_{n=3}, \beta)$ suggests that both $\beta \in [0.5, 1.1]$ can capture the minimum of $\mathcal{F}(E_{n=3}, \beta)$ and the BBC with high accuracy. In short, a faithful description of the NHSE should pay attention to not only the BBC but also the additional restrictions of the modified GBZ theory.

V. SUMMARY AND DISCUSSION

In summary, we found that the minimum of $\mathcal{F}(E, \beta)$ gives an interval instead of a single point, which eases the realization of BBC. Due to the extended choices of $\beta_{\min}$, a unified transformation coefficient β for samples with long-range hopping can be obtained. To compare the NHSE for different cases and eliminate the ambiguity, the strength of the NHSE is unified to the minimum of $|\beta_{\min} - 1|$. Notably, the modified GBZ theory under strong on-site disorders should fulfill two key points: (1) The transformation coefficient $\beta = \beta_{\min}$ should ensure the correctness of BBC by minimizing $\mathcal{F}(E, \beta)$; (2) $|\beta_{\min} - 1|$ should also be minimized. Finally, we clarified the paradox of the GBZ irrelevance of the NHSE under magnetic field with the help of the modified GBZ theory.

In disordered non-Hermitian systems, the modified GBZ theory means to find the minimum of $\mathcal{F}(E, \beta) = |\mathcal{F}_1(E) + \mathcal{F}_2(\beta)|$. We uncover that the relative quantity between $\mathcal{F}_1(E)$ and $\mathcal{F}_2(\beta)$ is very important. Here, $\mathcal{F}_1(E)$ has significant influences when the on-site disorder is strong enough. The global BBC can be realized for long-range hopping models, and the conventional GBZ irrelevance under magnetic field is also illuminated by considering $\mathcal{F}_1(E)$, which are distinct from the previous study [36]. Furthermore, the proposed min$[\mathcal{F}(E, \beta)]$ to achieve the BBC has no restriction on the concrete form of a Hamiltonian. Thus, the theoretical framework in our approach is quite universal for almost all the disordered non-Hermitian systems. In the Appendix C, we present two more prototypical examples, the non-Hermitian Su-Schrieffer-Heeger model [55] and the non-Hermitian Chern insulators [21], to illustrate the universality of our theory. Our work deepens the understanding of the characterization of the NHSE for samples with on-site disorders and extends the application of the GBZ theory.

ACKNOWLEDGMENTS

We are grateful for the valuable discussions with Q. Wei, S. Cheng, H. Liu, and J. Yu. This paper was supported by the National Key R&D Program of China (Grants No. 2019YFA0308403 and No. 2022YFA1403700), National Natural Science Foundation of China under Grants No. 12204044 and No. 12147126, and a Project Funded by the Priority Academic Program Development of Jiangsu Higher Education Institutions.

APPENDIX A: THE DERIVATION OF EQ. (6)

In this Appendix, we give the derivation of the analytical formula of $\mathcal{F}_1$. For Eq. (5), we mark $t^{+/-}$ as $(E - E_i) \neq 0$ since there is a high probability $t^{+/-} \sim (E - E_i)$. Here, we suppose E_i and E are the eigenvalues of $\mathcal{H}_{\mathrm{OBC};N-2\times N-2}$ and $\mathcal{H}_{\mathrm{OBC};N\times N}$, respectively. One should also notice that the eigenvalue of $\mathcal{H}_{\mathrm{OBC};N\times N}$ is also approximately the eigenvalue

of $\mathcal{H}_{\mathrm{OBC};N-2\times N-2}$, and only a slight deviation $\delta = |E_{\mathrm{OBC};N} - E_{\mathrm{OBC};N-2}| \to 0$ exists [36].

By considering δ, the analytical formula of $\mathcal{F}_1$ is obtained:

$$\ln(\mathcal{F}_1) \approx \sum_{i=1}^{N} \ln(E - E_i) = \lim_{\delta\to 0} \frac{N}{W}\left[\int_{-\frac{W}{2}}^{E-\delta} \ln(E-x)dx + \int_{E+\delta}^{\frac{W}{2}} \ln(E-x)dx\right]. \tag{A1}$$

In the above deviation, we require $E_i \to x$ and $|E - E_i| > \delta$ for $E_i \in [-\frac{W}{2}, \frac{W}{2}]$. Thus, one finally has

$$\ln(\mathcal{F}_1) = \ln\left\{\left[\left(E - \frac{W}{2}\right)^{[(1/2)-(E/W)]} \times \left(E + \frac{W}{2}\right)^{[(1/2)+(E/W)]} e^{-1}\right]^N\right\}. \tag{A2}$$

APPENDIX B: THE SIMILARITY BETWEEN A NON-HERMITIAN SYSTEM WITH A MAGNETIC FIELD AND A ONE-DIMENSIONAL MODEL WITH ON-SITE DISORDERS

In general, the similarity between a non-Hermitian system with a magnetic field and a one-dimensional model with on-site disorders can be identified based on the following considerations.

Firstly, they show a similar Hamiltonian formula. The Hamiltonian of a two-dimensional non-Hermitian rectangular lattice in the presence of a uniform perpendicular magnetic field with a irrational flux ϕ per unit cell is [37]

$$\mathcal{H} = \sum_{x,y} (t_x \pm \gamma) c^\dagger_{x,y} c_{x\pm\delta_x,y} + t_y e^{\pm i\phi x} c^\dagger_{x,y} c_{x,y\pm\delta_y}. \tag{B1}$$

The corresponding Harper Hamiltonian reads

$$\mathcal{H}(k_y) = \sum_x 2t_y \cos(k_y + \phi x) c^\dagger_{x,k_y} c_{x,k_y} + (t_x + \gamma) c^\dagger_{x,k_y} c_{x+\delta_x,k_y} + (t_x - \gamma) c^\dagger_{x,k_y} c_{x-\delta_x,k_y}, \tag{B2}$$

based on the Fourier transform $c_{x,k_y} = \sum_y \exp(-ik_y y) c_{x,y}$ [83]. This is a one-dimensional tight-binding model in which the quasiperiodicity appears as an on-site (diagonal) modulation. Due to the existence of a quasiperiodic potential $2t_y \cos(k_y + \phi x)$ [84], such a model looks similar to the models with on-site disorders, where the localization feature exists in principle.

Furthermore, the similarities can be clarified based on the proposed modified GBZ theory. Notably, the proposed modified GBZ theory is simplified to the calculation of a typical integral correlated to the disorder [see Eq. (A1)]. For Anderson disorder [86], it gives rise to

$$\int_{-W/2}^{W/2} P(\varepsilon_i) \ln(E - \varepsilon_i) d\varepsilon_i. \tag{B3}$$

Here, the random on-site energy for each site $\varepsilon_i \in [-W/2, W/2]$ satisfies the uniform distribution $P(\varepsilon_i) = \frac{1}{W}$ [87]. For the Harper model, the quasiperiodic potential $\varepsilon_x = 2t_y \cos(k_y + \phi x)$ is a composite function, i.e., $\frac{\varepsilon_x}{2t_y} = \cos(\Phi)$ ranging from -1 to 1. Here, $\Phi \in [0, 2\pi]$ and $P(\Phi) = \frac{1}{2\pi}$. The above integral becomes

$$\int_{-2t_y}^{2t_y} P(\varepsilon_x) \ln(E - \varepsilon_x) d\varepsilon_x. \tag{B4}$$

Here, $P(\varepsilon_x) = \frac{1}{2\pi\sqrt{(2t_y)^2 - (\varepsilon_x)^2}}$, which is similar to the on-site disorder cases.

Lastly, our theory is universal with a wide range of applicabilities for different forms of Hamiltonians. Thus, we can faithfully treat the quasiperiodic or random on-site potential with an equal footing within our theory of framework.

Based on the above considerations, a two-dimensional non-Hermitian model with a magnetic field can be roughly considered as a one-dimensional model with on-site disorders.

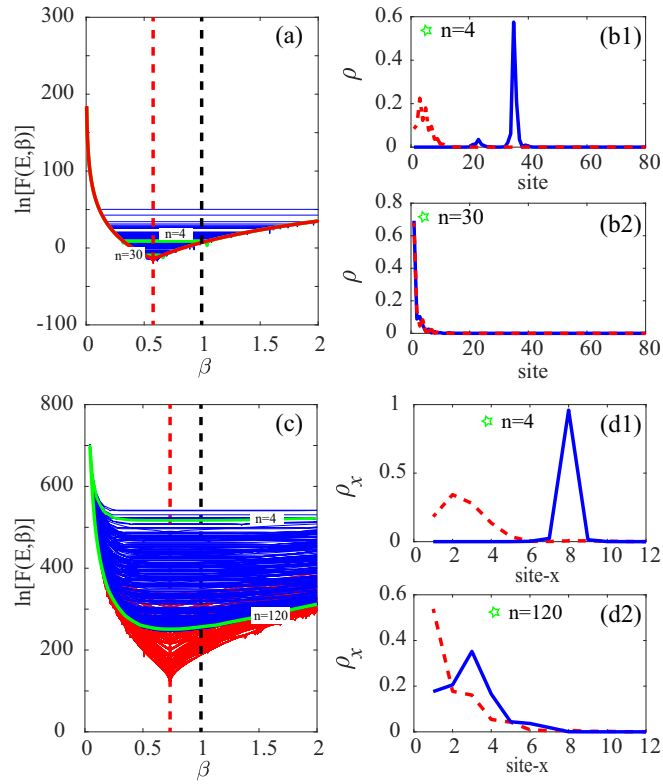

FIG. 4. (a) and (b) Non-Hermitian Su-Schrieffer-Heeger (SSH) model and (c) and (d) non-Hermitian Chern insulator. (a) The evolution of $\ln[\mathcal{F}(E,\beta)]$ with the increase of β for the non-Hermitian SSH model with $W = 0$ (red) and $W = 3$ (blue). The green lines are the cases of $n = 4$ (top) and $n = 30$ (bottom) under disorder, and dashed lines are $\beta = 1$ (black) and $\beta = \sqrt{(t_1 - \gamma)/(t_1 + \gamma)}$ (red). (b1) and (b2) Plots of eigenstates $\rho_n = |\psi_n|^2$ for $n = 4$ and 30, respectively. (c) and (d) are the same as (a) and (b), except $W = 10$ (blue), $n = 120$ (bottom), and $\rho_{x;n} = \sum_y |\psi_n(x,y)|^2$.

APPENDIX C: THE DISORDERED NON-HERMITIAN SU-SCHRIEFFER-HEEGER MODEL AND NON-HERMITIAN CHERN INSULATOR

To show the proposed theory is universal, we take two more typical models as examples.

The first one is the non-Hermitian Su-Schrieffer-Heeger (SSH) model [55]:

$$\begin{aligned}\mathcal{H} = &\sum_{i=1}^{N} \varepsilon_i (c_{i;A}^{\dagger} c_{i;A} + c_{i;B}^{\dagger} c_{i;B}) \\ &+ (t_1 + \gamma) c_{i;A}^{\dagger} c_{i;B} + (t_1 - \gamma) c_{i;B}^{\dagger} c_{i;A} \\ &+ t_2 c_{i;B}^{\dagger} c_{i+1;A} + t_2 c_{i+1;A}^{\dagger} c_{i;B}, \end{aligned} \tag{C1}$$

where $t_1 \pm \gamma$ and t_2 represent intracell and intercell hopping, respectively. Here, γ encodes the non-Hermitian strength. Also, $\varepsilon_i \in [-W/2, W/2]$ denotes the on-site disorder with W the disorder strength. Here, we fix $t_1 = 1, t_2 = 0.8, \gamma = 0.5$, and $N = 40$. According to the proposed modified GBZ theory, we plot the evolution of $\mathcal{F}(E, \beta)$ vs β, as shown in Fig. 4(a). For clean samples ($W = 0$, red), the minimum of $\mathcal{F}(E, \beta)$ is a single point $\beta_{\min} = \sqrt{(t_1 - \gamma)/(t_1 + \gamma)}$ (red dashed line), which agrees with the GBZ theory. Thus, $\beta_{\min}$ can rebuild the BBC and characterize the NHSE. When disorder is strong enough (blue), the plateau for the minimum of $\ln[\mathcal{F}(E, \beta)]$ exists, and an interval $\beta_{\min} \in [\Delta^-, \Delta^+]$ replaces a single point $\beta_{\min}$ for the nth eigenvalue E_n ($\mathcal{H}\psi_n = E_n\psi_n$). Note that it is distinct from the result for $W = 0$. All $\beta_{\min} \in [\Delta^-, \Delta^+]$ can realize the BBC with considerable accuracy due to $\mathcal{F}(E, \beta_{\min}) \approx \mathcal{F}(E, \sqrt{(t_1 - \gamma)/(t_1 + \gamma)})$. Furthermore, $\min|\beta_{\min} - 1|$ can depict the NHSE best for $\beta_{\min} \in [\Delta^-, \Delta^+]$ according to our theory. Here, $\min|\beta_{\min} - 1| = 0$ means the NHSE disappears due to localization of the skin mode caused by disorder. For clarity, we take $n = 4$ and 30 as two typical examples [see Figs. 4(b1) and 4(b2)]. When disorder is absent (red), the features of the NHSE remain for both states. However, the NHSE for $n = 4$ is destroyed, while $n = 30$ is almost unaffected after considering disorder strength $W = 3$ (blue). It is consistent with Fig. 4(a): $\min|\beta_{\min} - 1| = 0$ due to the right boundary of the plateau $\Delta^+ > 1$ for the eigenstate $n = 4$ (top green line), but $\min|\beta_{\min} - 1| \neq 0$ for $n = 30$ (bottom green line).

Next, we also study the non-Hermitian Chern insulator [21]. The corresponding Hamiltonian reads

$$\begin{aligned}\mathcal{H} = &\sum_{x,y} [(m+2)\sigma_z + \varepsilon_{x,y}\sigma_0] c_{x,y}^{\dagger} c_{x,y} \\ &+ \left[(t_1 + \gamma) \left(\frac{-\sigma_z - i\sigma_x}{2} \right) \right] c_{x,y}^{\dagger} c_{x+e_x,y} \\ &+ \left[(t_1 - \gamma) \left(\frac{-\sigma_z + i\sigma_x}{2} \right) \right] c_{x,y}^{\dagger} c_{x-e_x,y} \\ &+ \left[(t_2 + \gamma) \left(\frac{-\sigma_z - i\sigma_y}{2} \right) \right] c_{x,y}^{\dagger} c_{x,y+e_y} \\ &+ \left[(t_2 - \gamma) \left(\frac{-\sigma_z + i\sigma_y}{2} \right) \right] c_{x,y}^{\dagger} c_{x,y-e_y}, \end{aligned} \tag{C2}$$

where $\varepsilon_{x,y} \in [-W/2, W/2]$ denotes the on-site disorder with W the disorder strength. Here, we fix $m = 1, t_1 = t_2 = 1, \gamma = 0.3$, and $N = 12$. As shown in Figs. 4(c) and 4(d), the minimum of $\mathcal{F}(E, \beta)$ becomes the plateau with $\beta_{\min} \in [\Delta^-, \Delta^+]$ due to on-site disorder. Taking $n = 4$ and 120 as examples (green lines), some features can be identified. The NHSE of the mode $n = 4$ is destroyed for $\Delta^+ > 1$. These results are similar to the non-Hermitian SSH model. Therefore, the proposed modified GBZ theory is highly universal and can be adopted to achieve a systematic understanding of the NHSE in non-Hermitian systems.

[1] Y. Ashida, Z. P. Gong, and M. Ueda, Non-Hermitian physics, Adv. Phys. **69**, 249 (2020).

[2] F. K. Kunst and V. Dwivedi, Non-Hermitian systems and topology: A transfer-matrix perspective, Phys. Rev. B **99**, 245116 (2019).

[3] T. Helbig, T. Hofma, S. Imhof, M. Abdelghany, T. Kiessling, L. W. Molenkamp, C. H. Lee, A. Szameit, M. Greiter, and R. Thomale, Generalized bulk-boundary correspondence in non-Hermitian topolectrical circuits, Nat. Phys. **16**, 747 (2020).

[4] R. El-Ganainy, K. G. Makris, M. Khajavikhan, Z. H. Musslimani, S. Rotter, and D. N. Christodoulides, Non-Hermitian physics and PT symmetry, Nat. Phys. **14**, 11 (2018).

[5] T. E. Lee, Anomalous Edge State in a Non-Hermitian Lattice, Phys. Rev. Lett. **116**, 133903 (2016).

[6] K. Wang, A. Dutt, C. C. Wojcik, and S. H. Fan, Topological complex-energy braiding of non-Hermitian bands, Nature (London) **598**, 59 (2021).

[7] E. Edvardsson, F. K. Kunst, T. Yoshida, and E. J. Bergholtz, Phase transitions and generalized biorthogonal polarization in non-Hermitian systems, Phys. Rev. Res. **2**, 043046 (2020).

[8] M. Ezawa, Non-Hermitian higher-order topological states in nonreciprocal and reciprocal systems with their electric-circuit realization, Phys. Rev. B **99**, 201411(R) (2019).

[9] Z. S. Yang, K. Zhang, C. Fang, and J. P. Hu, Non-Hermitian Bulk-Boundary Correspondence and Auxiliary Generalized Brillouin Zone Theory, Phys. Rev. Lett. **125**, 226402 (2020).

[10] A. Ghatak and T. Das, New topological invariants in non-Hermitian systems, J. Phys.: Condens. Matter **31**, 263001 (2019).

[11] V. M. Martinez Alvarez, J. E. Barrios Vargas, M. Berdakin, and L. E. F. Foa Torres, Topological states of non-Hermitian systems, Eur. Phys. J. Spec. Top. **227**, 1295 (2018).

[12] Z. P. Gong, Y. Ashida, K. Kawabata, K. Takasan, S. Higashikawa, and M. Ueda, Topological Phases of Non-Hermitian Systems, Phys. Rev. X **8**, 031079 (2018).

[13] J. Y. Lee, J. Ahn, H. Zhou, and A. Vishwanath, Topological Correspondence between Hermitian and Non-Hermitian Systems: Anomalous Dynamics, Phys. Rev. Lett. **123**, 206404 (2019).

[14] D. Leykam, K. Y. Bliokh, C. Huang, Y. D. Chong, and F. Nori, Edge Modes, Degeneracies, and Topological Numbers in Non-Hermitian Systems, Phys. Rev. Lett. **118**, 040401 (2017).

[15] D. S. Borgnia, A. J. Kruchkov, and R. J. Slager, Non-Hermitian Boundary Modes and Topology, Phys. Rev. Lett. **124**, 056802 (2020).

[16] T. Liu, Y. R. Zhang, Q. Ai, Z. P. Gong, K. Kawabata, M. Ueda, and F. Nori, Second-Order Topological Phases in Non-Hermitian Systems, Phys. Rev. Lett. **122**, 076801 (2019).

[17] Ken Shiozaki and S. Ono, Symmetry indicator in non-Hermitian systems, Phys. Rev. B **104**, 035424 (2021).

[18] C. H. Liu, H. Jiang, and S. Chen, Topological classification of non-Hermitian systems with reflection symmetry, Phys. Rev. B **99**, 125103 (2019).

[19] K. Kawabata, K. Shiozaki, M. Ueda, and M. Sato, Symmetry and Topology in Non-Hermitian Physics, Phys. Rev. X **9**, 041015 (2019).

[20] F. Song, S. Y. Yao, and Z. Wang, Non-Hermitian Topological Invariants in Real Space, Phys. Rev. Lett. **123**, 246801 (2019).

[21] S. Yao, F. Song, and Z. Wang, Non-Hermitian Chern Bands, Phys. Rev. Lett. **121**, 136802 (2018).

[22] H. T. Shen, B. Zhen, and L. Fu, Topological Band Theory for Non-Hermitian Hamiltonians, Phys. Rev. Lett. **120**, 146402 (2018).

[23] K. Wang, A. Dutt, K. Y. Yang, C. C. Wojcik, J. Vuckovic, and S. Fan, Generating arbitrary topological windings of a non-Hermitian band, Science **371**, 1240 (2021).

[24] T. S. Deng and W. Yi, Non-Bloch topological invariants in a non-Hermitian domain wall system, Phys. Rev. B **100**, 035102 (2019).

[25] S. Liu, S. J. Ma, C. Yang, L. Zhang, W. L. Gao, Y. J. Xiang, T. J. Cui, and S. Zhang, Gain-and loss-induced topological insulating phase in a non-Hermitian electrical circuit, Phys. Rev. Appl. **13**, 014047 (2020).

[26] Q. B. Zeng and Y. Xu, Winding numbers and generalized mobility edges in non-Hermitian systems, Phys. Rev. Res. **2**, 033052 (2020).

[27] J. Claes and T. L. Hughes, Skin effect and winding number in disordered non-Hermitian systems, Phys. Rev. B **103**, L140201 (2021).

[28] X. L. Luo, Z. Y. Xiao, K. Kawabata, T. Ohtsuki, R. Shindou, Unifying the Anderson transitions in Hermitian and non-Hermitian systems, Phys. Rev. Res. **4**, L022035 (2022).

[29] D.-W. Zhang, L.-Z. Tang, L.-J. Lang, H. Yan, and S.-L. Zhu, Non-Hermitian topological Anderson insulators, Sci. China-Phys. Mech. Astron. **63**, 267062 (2020).

[30] X. L. Luo, T. Ohtsuki, and R. Shindou, Universality Classes of the Anderson Transitions Driven by Non-Hermitian Disorder, Phys. Rev. Lett. **126**, 090402 (2021).

[31] H. F. Liu, Z. X. Su, Z. Q. Zhang, and H. Jiang, Topological Anderson insulator in two-dimensional non-Hermitian systems, Chin. Phys. B **29**, 050502 (2020).

[32] Y. Huang and B. I. Shklovskii, Anderson transition in three-dimensional systems with non-Hermitian disorder, Phys. Rev. B **101**, 014204 (2020).

[33] A. F. Tzortzakakis, K. G. Makris, and E. N. Economou, Non-Hermitian disorder in two-dimensional optical lattices, Phys. Rev. B **101**, 014202 (2020).

[34] L. Z. Tang, L. F. Zhang, G. Q. Zhang, and D. W. Zhang, Topological Anderson insulators in two-dimensional non-Hermitian disordered systems, Phys. Rev. A **101**, 063612 (2020).

[35] H. F. Liu, J. K. Zhou, B. L. Wu, Z. Q. Zhang, and H. Jiang, Real-space topological invariant and higher-order topological Anderson insulator in two-dimensional non-Hermitian systems, Phys. Rev. B **103**, 224203 (2021).

[36] Z.-Q. Zhang, H. Liu, H. Liu, H. Jiang, and X. C. Xie, Bulk-boundary correspondence in disordered non-Hermitian systems, Sci. Bull. **68**, 157 (2023).

[37] M. Lu, X. X. Zhang, and M. Franz, Magnetic Suppression of Non-Hermitian Skin Effects, Phys. Rev. Lett. **127**, 256402 (2021).

[38] K. Shao, Z. T. Cai, H. Geng, W. Chen, and D. Y. Xing, Cyclotron quantization and mirror-time transition on nonreciprocal lattices, Phys. Rev. B **106**, L081402 (2022).

[39] Y. Peng, J. Jie, D. Yu, and Y. Wang, Manipulating non-Hermitian skin effect via electric fields, Phys. Rev. B **106**, L161402 (2022).

[40] E. J. Bergholtz, J. C. Budich, and F. K. Kunst, Exceptional topology of non-Hermitian systems, Rev. Mod. Phys. **93**, 015005 (2021).

[41] J. C. Budich, J. Carlström, F. K. Kunst, and E. J. Bergholtz, Symmetry-protected nodal phases in non-Hermitian systems, Phys. Rev. B **99**, 041406(R) (2019).

[42] J. Carlström and E. J. Bergholtz, Exceptional links and twisted Fermi ribbons in non-Hermitian systems, Phys. Rev. A **98**, 042114 (2018).

[43] J. Carlström, M. Stålhammar, J. C. Budich, and E. J. Bergholtz, Knotted non-Hermitian metals, Phys. Rev. B **99**, 161115(R) (2019).

[44] R. Okugawa and T. Yokoyama, Topological exceptional surfaces in non-Hermitian systems with parity-time and parity-particle-hole symmetries, Phys. Rev. B **99**, 041202(R) (2019).

[45] Z. S. Yang, A. P. Schnyder, J. P. Hu, C. K. Chiu, Fermion Doubling Theorems in Two-Dimensional Non-Hermitian Systems for Fermi Points and Exceptional Points, Phys. Rev. Lett. **126**, 086401 (2021).

[46] Z. Yang and J. Hu, Non-Hermitian Hopf-link exceptional line semimetals, Phys. Rev. B **99**, 081102(R) (2019).

[47] W. Zhu, X. Fang, D. Li, Y. Sun, Y. Li, Y. Jing, and H. Chen, Simultaneous Observation of a Topological Edge State and Exceptional Point in an Open and Non-Hermitian Acoustic System, Phys. Rev. Lett. **121**, 124501 (2018).

[48] H. P. Hu and E. H. Zhao, Knots and Non-Hermitian Bloch Bands, Phys. Rev. Lett. **126**, 010401 (2021).

[49] K. Yokomizo and S. Murakami, Topological semimetal phase with exceptional points in one-dimensional non-Hermitian systems, Phys. Rev. Res. **2**, 043045 (2020).

[50] W. Hu, H. Wang, P. P. Shum, and Y. D. Chong, Exceptional points in a non-Hermitian topological pump, Phys. Rev. B **95**, 184306 (2017).

[51] V. M. Martinez Alvarez, J. E. B. Vargas, and L. E. F. F. Torres, Non-Hermitian robust edge states in one dimension: Anomalous localization and eigenspace condensation at exceptional points, Phys. Rev. B **97**, 121401(R) (2018).

[52] K. Sone, Y. Ashida, and T. Sagawa, Exceptional non-Hermitian topological edge mode and its application to active matter, Nat. Commun. **11**, 5745 (2020).

[53] L. H. Li and C. H. Lee, Non-Hermitian pseudo-gaps, Sci. Bull. **67**, 685 (2022).

[54] N. Matsumoto, K. Kawabata, Y. Ashida, S. Furukawa, and M. Ueda, Continuous Phase Transition without Gap Closing in Non-Hermitian Quantum Many-Body Systems, Phys. Rev. Lett. **125**, 260601 (2020).

[55] S. Y. Yao and Z. Wang, Edge States and Topological Invariants of Non-Hermitian Systems, Phys. Rev. Lett. **121**, 086803 (2018).
[56] F. K. Kunst, E. Edvardsson, J. C. Budich, and E. J. Bergholtz, Biorthogonal Bulk-Boundary Correspondence in Non-Hermitian Systems, Phys. Rev. Lett. **121**, 026808 (2018).
[57] K. Yokomizo and S. Murakami, Non-Bloch Band Theory of Non-Hermitian Systems, Phys. Rev. Lett. **123**, 066404 (2019).
[58] F. Song, S. Y. Yao, and Z. Wang, Non-Hermitian Skin Effect and Chiral Damping in Open Quantum Systems, Phys. Rev. Lett. **123**, 170401 (2019).
[59] Y. Xiong, Why does bulk boundary correspondence fail in some non-Hermitian topological models, J. Phys. Commun. **2**, 035043 (2018).
[60] C. H. Lee and R. Thomale, Anatomy of skin modes and topology in non-Hermitian systems, Phys. Rev. B **99**, 201103(R) (2019).
[61] K. Zhang, Z. Yang, and C. Fang, Correspondence between Winding Numbers and Skin Modes in Non-Hermitian Systems, Phys. Rev. Lett. **125**, 126402 (2020).
[62] L. H. Li, C. H. Lee, S. Mu, and J. B. Gong, Critical non-Hermitian skin effect, Nat. Commun. **11**, 5491 (2020).
[63] N. Okuma, K. Kawabata, K. Shiozaki, and M. Sato, Topological Origin of Non-Hermitian Skin Effects, Phys. Rev. Lett. **124**, 086801 (2020).
[64] X. Q. Sun, P. H. Zhu, and T. L. Hughes, Geometric Response and Disclination-Induced Skin Effects in Non-Hermitian Systems, Phys. Rev. Lett. **127**, 066401 (2021).
[65] S. Liu, R. W. Shao, S. J. Ma, L. Zhang, O. B. You, H. T. Wu, Y. J. Xiang, T. J. Cui, and S. Zhang, Non-Hermitian skin effect in a non-Hermitian electrical circuit, Research **2021**, 5608038 (2021).
[66] K. Kawabata, M. Sato, and K. Shiozaki, Higher-order non-Hermitian skin effect, Phys. Rev. B **102**, 205118 (2020).
[67] Y. F. Yi and Z. S. Yang, Non-Hermitian Skin Modes Induced by On-Site Dissipations and Chiral Tunneling Effect, Phys. Rev. Lett. **125**, 186802 (2020).
[68] C. X. Guo, C. H. Liu, X. M. Zhao, Y. Liu, and S. Chen, Exact Solution of Non-Hermitian Systems with Generalized Boundary Conditions: Size-Dependent Boundary Effect and Fragility of the Skin Effect, Phys. Rev. Lett. **127**, 116801 (2021).
[69] C. Yuce, Non-Hermitian anomalous skin effect, Phys. Lett. A **384**, 126094 (2020).
[70] Y. X. Fu, J. H. Hu, and S. L. Wan, Non-Hermitian second-order skin and topological modes, Phys. Rev. B **103**, 045420 (2021).
[71] K. Yokomizo and S. Murakami, Scaling rule for the critical non-Hermitian skin effect, Phys. Rev. B **104**, 165117 (2021).
[72] R. Okugawa, R. Takahashi, and K. Yokomizo, Second-order topological non-Hermitian skin effects, Phys. Rev. B **102**, 241202(R) (2020).
[73] X. Y. Zhu, H. Q. Wang, S. K. Gupta, H. J. Zhang, B. Xie, M. H. Lu, and Y. F. Chen, Photonic non-Hermitian skin effect and non-Bloch bulk-boundary correspondence, Phys. Rev. Res. **2**, 013280 (2020).
[74] X. Zhang, Y. Tian, J.-H. Jiang, M.-H. Lu, and Y.-F. Chen, Observation of higher-order non-Hermitian skin effect, Nat. Commun. **12**, 5377 (2021).
[75] K. Zhang, Z. S. Yang, and C. Fang, Universal non-Hermitian skin effect in two and higher dimensions, Nat. Commun. **13**, 2496 (2022).
[76] N. Okuma and M. Sato, Non-Hermitian Skin Effects in Hermitian Correlated or Disordered Systems: Quantities Sensitive or Insensitive to Boundary Effects and Pseudo-Quantum-Number, Phys. Rev. Lett. **126**, 176601 (2021).
[77] Y. Song, W. Liu, L. Zheng, Y. Zhang, B. Wang, and P. Lu, Two-Dimensional Non-Hermitian Skin Effect in a Synthetic Photonic Lattice, Phys. Rev. Appl. **14**, 064076 (2020).
[78] S. Longhi, Non-Hermitian skin effect beyond the tight-binding models, Phys. Rev. B **104**, 125109 (2021).
[79] H. W. Li, X. L. Cui, and W. Yi, Non-Hermitian skin effect in a spin-orbit-coupled Bose-Einstein condensate, JUSTC **52**, 2 (2022).
[80] C. H. Lee, L. Li, and J. B. Gong, Hybrid Higher-Order Skin-Topological Modes in Nonreciprocal Systems, Phys. Rev. Lett. **123**, 016805 (2019).
[81] R. Sarkar, S. S. Hegde, and A. Narayan, Interplay of disorder and point-gap topology: Chiral modes, localization, and non-Hermitian Anderson skin effect in one dimension, Phys. Rev. B **106**, 014207 (2022).
[82] Y. E. Kraus, Y. Lahini, Z. Ringel, M. Verbin, and O. Zilberberg, Topological States and Adiabatic Pumping in Quasicrystals, Phys. Rev. Lett. **109**, 106402 (2012).
[83] Y. E. Kraus and O. Zilberberg, Topological Equivalence between the Fibonacci Quasicrystal and the Harper Model, Phys. Rev. Lett. **109**, 116404 (2012).
[84] D. R. Grempel, S. Fishman, and R. E. Prange, Localization in an Incommensurate Potential: An Exactly Solvable Model, Phys. Rev. Lett. **49**, 833 (1982).
[85] N. Hatano and D. R. Nelson, Localization Transitions in Non-Hermitian Quantum Mechanics, Phys. Rev. Lett. **77**, 570 (1996).
[86] P. W. Anderson, Absence of diffusion in certain random lattices, Phys. Rev. **109**, 1492 (1958).
[87] D. Vollhardt and P. Wölfle, Self-consistent theory of Anderson localization, Mod. Probl. Condens. Matter Sci. **32**, 1 (1992).